

Memory-function approach to spin-temperature oscillations in the rotating frame

U. Deininghaus and M. Mehring

Institut für Physik, Universität Dortmund, 4600 Dortmund 50, Germany

(Received 10 November 1980)

A memory-function approach (Mori-Zwanzig-Shimizu) is applied to treat the non-Markovian behavior of coupled nuclear spins in the spin-locking experiment. One-, two-, and three-spin-temperature concepts are discussed and compared with experimental results for ^{19}F in CaF_2 .

I. INTRODUCTION

The spin interactions in solids containing either nuclear or electron spins can be separated into spin-spin interactions and spin-lattice interactions, respectively.^{1,2} We shall restrict ourselves in this article to the former, namely, to the dipolar interaction of nuclear spins in a large static magnetic field H_0 .

The separation into spin-spin and spin-lattice interactions is justified by the two different time scales (usually T_2 and T_1) involved, where in the solid state usually $T_2 \ll T_1$, i.e., the spins are effectively disconnected from the lattice on the time scale of spin-spin interactions (T_2).

The experiments we are going to discuss, however, are of some importance for the evaluation of spin-lattice relaxation measurements in the rotating frame.³

Due to the many-body character of the spin-spin interactions, the theoretical treatment of spin dynamics is quite involved and no rigorous answer is expected. Different kinds of approximation schemes have been applied in the past, ranging from moment expansions to integrodifferential equation approaches of different sorts. The current literature has mainly been restricted to the free-induction decay and to the so-called Strombotne-Hahn experiment.⁴ In the following we shall discuss the spin-locking experiment for the following reasons: (i) it offers a rather general model for mixing processes between subsystems of a many-body system; (ii) it contains the free-induction decay (fid) as a limiting case; (iii) it is the experimental technique widely applied in nuclear magnetic resonance (NMR) for the observation of spin-lattice relaxation in the rotating frame ($T_{1\rho}$) (Ref. 3); and (iv) there is a pulsed analog version of spin locking which has stirred up some interest recently.⁵

The spin-locking experiment was first proposed and performed by Solomon.⁶ It consists of, e.g., applying a 90°_y pulse in the rotating frame to a spin system in Boltzmann equilibrium, thus creating macroscopic magnetization in the x direction, which is "locked" by an rf field of strength H_1 in the same direction

(x) in the rotating frame. Terminating the H_1 field after a time τ leads to a free-induction decay (fid), whose amplitude is a measure of the magnetization $M_x(\tau)$, i.e., of the "Zeeman order" in the x direction of the rotating frame. Such a sequence is sketched in Fig. 1. Moreover one is interested in the dynamic behavior of "dipolar order" during spin locking. In fact, the dipolar order at the termination time τ of the H_1 field is unaffected by the fid and can be observed by means of a 45° read-out pulse after the fid,⁷ as is sketched in Fig. 1.

The following relevant features as a function of τ are observed and have been known for some time^{8,9}: (i) oscillations with frequency $2\omega_1$ (where $\omega_1 = \gamma H_1$) with a damping time of the order T_2 (spin-spin relaxation time) and (ii) decay of the magnetization to a constant value, depending on H_1 and the "local field" H_L due to spin-spin interaction. For high field ($H_1/H_L \gg 1$) this decay takes place in two different time domains; the first domain is terminated with the disappearance of the oscillations in (i), while the second occurs on a much slower time scale.

The final magnetization in a spin-locking experiment is readily calculable by simple spin thermodynamics.² After the 90°_y pulse we start with an initial density matrix in the frame rotating at the Larmor frequency ω_0 as²

$$\rho_0 \approx 1 - \alpha_0 \mathcal{J}_x, \quad (1.1)$$

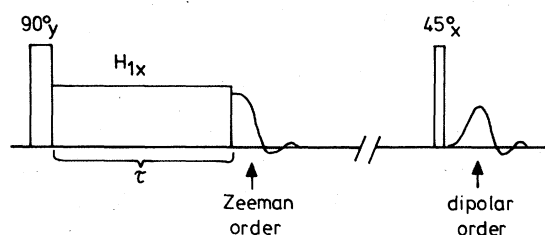


FIG. 1. Spin-locking pulse sequence for detection of Zeeman and dipolar order as a function of H_{1x} and τ . The time delay between the 90°_y pulse and the 45°_x pulse is at about $t^* \approx 400 \mu\text{s}$ so that $T_2 \ll t^* \ll T_{1D}$.

with $\alpha_0 = (1/k_B T_L) \omega_0/\omega_1$ (where k_B is the Boltzmann constant and T_L is the lattice temperature), $\mathcal{H}_x = \omega_1 I_x$, and where the high-temperature approximation has been invoked as is usually done in NMR. Under the action of the Hamiltonian

$$\mathcal{H} = \mathcal{H}_x + \mathcal{H}_{DZ} \quad (1.2)$$

where \mathcal{H}_{DZ} is the secular part of the dipolar Hamiltonian with

$$\mathcal{H}_{D\alpha} = \frac{1}{2} \sum_{i \neq j} A_{ij} (3I_{\alpha i} I_{\alpha j} - \bar{I}_i \cdot \bar{I}_j) \quad (1.3)$$

$$\alpha = x, y, z \quad , \quad A_{ij} = \gamma^2 \hbar \frac{1 - 3 \cos^2 \theta_{ij}}{r_{ij}^3} \quad ,$$

the initial density matrix ρ_0 evolves into the final state

$$\rho_f = 1 - \alpha_f \mathcal{H} \quad (1.4)$$

The "inverse temperature" α_f may be calculated by assuming energy conservation²

$$\alpha_f = \alpha_0 \frac{\omega_1^2}{\omega_1^2 + \omega_L^2} \quad (1.5)$$

where ω_L is the frequency of the local field

$$\frac{\omega_1^2}{\omega_L^2} = \frac{\text{tr}(\mathcal{H}_x^2)}{\text{tr}(\mathcal{H}_{DZ}^2)} \quad (1.6)$$

Physically this decay of magnetization signals an equilibration of the temperatures of the Zeeman and the dipolar reservoir, a process, which is generally known as "mixing."

The above calculation is typical for spin thermodynamics. It gives us, however, no information about what happens between the initial and the final state. Also the Provotorov theory¹⁰ fails to describe the dynamics involved, since in our case there is no weak perturbation which mixes the two reservoirs. In contrast, the appearance of oscillations with frequency $2\omega_1$, is a manifestation of the non-Markovian behavior of the mixing process which makes it necessary to consider the general equation of motion.

Several approaches have been devised for the description of systems with strong coupling. The first one, mainly due to Prigogine and co-workers, starts with a microscopic approach using partial resummation in perturbation theory up to infinite order.¹¹ This approach is quite laborious and the results, as compared with the invested labor, are not overwhelming. The second approach, which is a more naive one, uses some explicitly calculable moments of the correlation function, fitting them to a line shape which is usually Gaussian or Lorentzian.² And last but not least we want to mention Mori's approach,¹² which expands the correlation function into an infinite-order continued fraction and tries to obtain the correct short- and long-time behavior by suit-

able (but often not rigorously justifiable) approximations. This formalism has rarely been applied so far to NMR.¹³

The purpose of this paper is twofold. First we want to derive exact equations of motion for the Zeeman energy and the secular and nonsecular dipolar energies in the rotating frame. In Sec. II we employ a projection scheme due to Mori, Zwanzig, and Shimizu to derive rigorous equations of motion for the corresponding "inverse temperatures" within a one-, two-, and three-temperature concept, respectively.

Secondly, we want to demonstrate, that experimental data can be theoretically described most conveniently using no adjustable parameter whatsoever, by assuming a simple functional form for the memory functions involved. The lattice structure enters in this approach through second and fourth moment-type calculations. The corresponding experimental and theoretical results are discussed in Sec. III.

We want to emphasize, that our approach is more rigorous and offers more physical insight than the naive direct fitting of the time dependence of the Zeeman order by, e.g., a Gaussian having the correct second moment as was applied to the Strombotne-Hahn experiment.²

II. THEORY OF SPIN-LOCKING EXPERIMENT

A. Equations of motion

All information about macroscopic observables may be extracted from the density matrix of the system which obeys the Liouville-von Neumann equation:

$$\frac{d}{dt} |\rho\rangle = -i \hat{\mathcal{H}} |\rho\rangle \quad (2.1)$$

In the following we will adopt the notation of Liouville space, i.e., we define

(i) a superoperator $\hat{\mathcal{H}}$

$$\hat{\mathcal{H}} |\rho\rangle = |[\mathcal{H}, \rho]\rangle \quad (2.2)$$

(ii) a scalar product

$$(A | B) = \text{tr}(A^\dagger B) \quad (2.3)$$

The Liouville-von Neumann equation (2.1), however, is not exactly solvable except in trivial or pathological cases. Nevertheless, this may not be necessary, since we are only interested in those parts of $\rho(t)$, that correspond to macroscopic observable quantities, i.e., in our case to Zeeman and dipolar order.

Projection schemes have long been known in statistical mechanics,^{14,15} but we will restrict ourselves to a version that is amenable to NMR. This version was introduced by Shimizu¹⁶ and by Lado, Memory,

and Parker¹⁷ and has been used in the dynamical theory of high-resolution NMR in solids^{18,19} recently.

As usual, we project out the relevant variables

$$\rho = P\rho + (1-P)\rho, \quad (2.4)$$

with the projection operator

$$P = \sum_{i=1}^N \frac{|Q_i\rangle\langle Q_i|}{(Q_i|Q_i)} \quad (2.5)$$

on the relevant variables Q_i . The equations of motions are greatly simplified if we assume the Q_i to be pairwise orthogonal

$$(Q_i|Q_j) = 0 \text{ for } i \neq j. \quad (2.6)$$

The macroscopic observables are now related to so-called thermodynamic coordinates $\beta_i(t)$

$$\rho(t) = \sum_{i=1}^N \beta_i(t) Q_i + (1-P)\rho(t), \quad (2.7)$$

which obey the following *exact* non-Markovian kinetic equations

$$\begin{aligned} \frac{d}{dt}\beta_k = & -i \sum_{j=1}^N (Q_k|\hat{\mathcal{K}}|Q_j)\beta_j \\ & - i \frac{(Q_k|\hat{\mathcal{K}}\hat{S}(t,0)(1-P)|\rho(0))}{(Q_k|Q_k)} \\ & - \sum_{j=1}^N \int_0^t K_{kj}(t,t')\beta_j(t') dt', \end{aligned} \quad (2.8)$$

with the so-called memory functions

$$K_{kj}(t,t') = \frac{(Q_k|\hat{\mathcal{K}}(t)\hat{S}(t,t')(1-P)\hat{\mathcal{K}}(t')|Q_j)}{(Q_k|Q_k)} \quad (2.9)$$

and

$$S(t,t') = T \exp\left[-i \int_{t'}^t d\tau (1-P)\hat{\mathcal{K}}(\tau)\right]. \quad (2.10)$$

In the following we will refer to the thermodynamic coordinates β_i as to "inverse temperatures" or even more loosely to "temperatures" although nondiagonal elements of the density matrix are involved and are taken into account rigorously.

Our main task now is to calculate the memory functions K_{kj} .²⁰ They are, however, not exactly calculable in most cases (nor is the Liouville-von Neumann equation), but one hopes that approximations to the memory functions, such as functional assumptions or continued fraction approximations,^{21,22} will be less drastic than applying these techniques to the original equation of motion (2.1). Some general

properties of K_{kj} may be stated.^{14-16,23}

(i) Symmetry:

$$K_{kj}(t,t') = K_{jk}^*(t',t) \frac{(Q_j|Q_j)}{(Q_k|Q_k)}; \quad (2.11)$$

(ii) Boundedness:

$$|K_{kj}|^2 \leq \frac{(Q_k|\hat{\mathcal{K}}^2|Q_k)}{(Q_k|Q_k)} \frac{(Q_j|\hat{\mathcal{K}}^2|Q_j)}{(Q_j|Q_j)}; \quad (2.12)$$

(iii) Completeness: If P projects on all variables that are contained in the Hamiltonian, i.e.,

$$P = \sum_{i=1}^N \frac{|Q_i\rangle\langle Q_i|}{(Q_i|Q_i)}, \quad \hat{\mathcal{K}} = \sum_{i=1}^N Q_i$$

then

$$\sum_{j=1}^N K_{ij}(t) = 0. \quad (2.13)$$

Let us now turn to the spin-locking experiment. First we have to determine the relevant variables which are also experimentally observable and which have to be included in the projection operator.

B. One-temperature concept

In the usual spin-locking experiment (as employed in $T_{1\rho}$ measurements) one is predominantly interested in the time evolution of the transverse magnetization, i.e.,

$$\langle I_x(t) \rangle = \text{tr}[\rho(t)I_x]$$

so that we may first consider the following form of the density matrix

$$\rho(t) = 1 - \alpha(t)\mathcal{K}_x + \dots, \quad (2.14)$$

leading to the projection operator

$$P = P_x = \frac{|\mathcal{K}_x\rangle\langle\mathcal{K}_x|}{(\mathcal{K}_x|\mathcal{K}_x)} \quad (2.15)$$

and to the equation of motion

$$\frac{d\alpha}{dt} = - \int_0^t K(t-t')\alpha(t') dt', \quad (2.16)$$

where

$$K(t) = \frac{(\mathcal{K}_x|\hat{\mathcal{K}}_{DZ} \exp[-it(1-P)\hat{\mathcal{K}}]\hat{\mathcal{K}}_{DZ}|\mathcal{K}_x)}{(\mathcal{K}_x|\mathcal{K}_x)} \quad (2.17)$$

A moment expansion of $K(t)$ leads to

$$K(t) = M_2 \left[1 - \frac{t^2}{2} \left(\frac{M_4 - M_2^2}{M_2} + 4\omega_1^2 \right) + \frac{t^4}{4!} \left(\frac{M_6 - 2M_4M_2 + M_2^3}{M_2} + 8\omega_1^2 \frac{M_4 - M_2^2}{M_2} + 16\omega_1^2 \frac{\tilde{M}_4}{M_2} + 16\omega_1^4 \right) \dots \right], \quad (2.18a)$$

where M_2, M_4, M_6 are the second, fourth, and sixth moment of the free-induction decay (fid) line shape¹ and \tilde{M}_4 is a modified fourth moment defined by

$$\begin{aligned} \tilde{M}_4 &= (\mathfrak{J}\mathfrak{C}_x | \mathfrak{J}\hat{\mathfrak{C}}_{\text{DZ}} (\mathfrak{J}\hat{\mathfrak{C}}_{\text{DX}}^2/4) \mathfrak{J}\hat{\mathfrak{C}}_{\text{DZ}} | \mathfrak{J}\mathfrak{C}_x) / (\mathfrak{J}\mathfrak{C}_x | \mathfrak{J}\mathfrak{C}_x) \\ &= \frac{3}{4} \left[\sum_j A_{jk}^4 I(I+1) \left(\frac{12}{5} I^2 + \frac{12}{5} I - \frac{9}{5} \right) + \sum_{k,l} A_{jk}^2 A_{jl}^2 4 I^2 (I+1)^2 + \sum_{k,l} A_{kl}^2 A_{jk} A_{jl} 8 I^2 (I+1)^2 \right]. \end{aligned} \quad (2.18b)$$

In order to obtain the overall line shape of $K(t)$, we now turn to the structure of the "propagator"

$$S(t) = \exp[-it(1-P)\mathfrak{J}\mathfrak{C}] ,$$

which allows some assumptions on the functional structure of $K(t)$ to be made.

First consider the "free" (i.e., undamped) propagator

$$S_{\text{free}}(t) = \exp(-it\mathfrak{J}\mathfrak{C}_x) , \quad (2.19)$$

$$\exp[-it(1-P)(\mathfrak{J}\mathfrak{C}_x + \mathfrak{J}\mathfrak{C}_{\text{DZ}})] = \exp(-it\mathfrak{J}\mathfrak{C}_x) T \exp \left[-i \int_0^t \exp(+it'\mathfrak{J}\mathfrak{C}_x) (1-P)\mathfrak{J}\mathfrak{C}_{\text{DZ}} \exp(-it'\mathfrak{J}\mathfrak{C}_x) dt' \right] .$$

The second factor (which leads to damping) may be approximated in the following cases.

(i) Low-field case ($\omega_1 \ll \omega_L$): Baker-Campbell-Hausdorff (BCH) formula²⁴

$$\exp[-it(1-P)\mathfrak{J}\mathfrak{C}] \simeq \exp(-it\mathfrak{J}\mathfrak{C}_x) \exp[-it(1-P_x)\mathfrak{J}\mathfrak{C}_{\text{DZ}}] \exp \left[\frac{t^2}{2} [\mathfrak{J}\mathfrak{C}_x, (1-P_x)\mathfrak{J}\mathfrak{C}_{\text{DZ}}] \right] ,$$

which yields

$$K(t) = M_2 \left[1 - \frac{M_4 - M_2^2}{M_2} \frac{t^2}{2} + \dots \right] \cos(2\omega_1 t) .$$

(ii) High-field case ($\omega_1 \gg \omega_L$): Magnus formula²⁴ together with the cycle-time approximation²⁵

$$\begin{aligned} e^{-it(1-P)\mathfrak{J}\mathfrak{C}} &= e^{-it\mathfrak{J}\mathfrak{C}_x} \\ &\times T \exp \left[-i \int_0^t e^{+it'\mathfrak{J}\mathfrak{C}_x} (1-P)\mathfrak{J}\mathfrak{C}_{\text{DZ}} e^{-it'\mathfrak{J}\mathfrak{C}_x} dt' \right] \end{aligned}$$

and

$$\begin{aligned} T \exp \left[-i \int_0^t e^{+it'\mathfrak{J}\mathfrak{C}_x} (1-P)\mathfrak{J}\mathfrak{C}_{\text{DZ}} e^{-it'\mathfrak{J}\mathfrak{C}_x} dt' \right] \\ = \exp[-i(\bar{\mathfrak{J}}\mathfrak{C}_0 + \bar{\mathfrak{J}}\mathfrak{C}_1 + \dots)t] , \end{aligned}$$

where especially the 0th Magnus approximation is given by

$$\bar{\mathfrak{J}}\mathfrak{C}_0 = \frac{1}{t_c} \int_0^{t_c} e^{-it'\mathfrak{J}\mathfrak{C}_x} (1-P)\mathfrak{J}\mathfrak{C}_{\text{DZ}} e^{-it'\mathfrak{J}\mathfrak{C}_x} dt' , \quad (2.22)$$

with the cycle time

$$t_c = \frac{\pi}{\omega_1} \ll T_2 . \quad (2.23)$$

In our case we obtain

$$\bar{\mathfrak{J}}\mathfrak{C}_0 = -\frac{1}{2}\mathfrak{J}\mathfrak{C}_{\text{DX}} \quad (2.24)$$

which yields

$$K_{\text{free}}(t) = M_2 \cos(2\omega_1 t) . \quad (2.20)$$

The effect of $\mathfrak{J}\mathfrak{C}_{\text{DZ}}$ in $S(t)$ will be to cause some damping, so that $K(t)$ will be of the form

$$K(t) = g(t) \cos(2\omega_1 t) , \quad (2.21)$$

where $g(t)$ exhibits damping. Expanding around the exactly solvable K_{free} , we use the well-known identity

[for the definition of $\mathfrak{J}\mathfrak{C}_{\text{DX}}$, see Eq. (1.3)] which yields

$$K(t) \simeq M_2 \left[1 - \frac{\tilde{M}_4}{M_2} \frac{t^2}{2} + \dots \right] \cos(2\omega_1 t) . \quad (2.25)$$

Having eliminated the most rapidly varying factor in $K(t)$, we make a functional assumption for the damping factor $g(t)$.

In order to satisfy the conditions (2.11) and (2.12), we choose a Gaussian form of $g(t)$, as has been done by many authors.^{11,26} We are aware, however, that this choice is in conflict with the thermodynamic limit (1.5), since with a Gaussian choice for $g(t)$, $\alpha(t)$ will decay to zero. This discrepancy may be resolved in Mori's continued fraction formalism, as will be discussed in Sec. III D. If we restrict ourselves to the discussion of the short-time behavior, however, the Gaussian assumption may be justified. Adapting the half-width of $g(t)$ to yield the correct second moment of $K(t)$, we obtain

(i) low-field case ($\omega_1 \ll \omega_L$)

$$K(t) = M_2 \exp \left[-\frac{M_4 - M_2^2}{M_2} \frac{t^2}{2} \right] \cos(2\omega_1 t) , \quad (2.26)$$

(ii) high-field case ($\omega_1 \gg \omega_L$)

$$K(t) = M_2 \exp \left[-\frac{\tilde{M}_4}{M_2} \frac{t^2}{2} \right] \cos(2\omega_1 t) . \quad (2.27)$$

C. Two-temperature concept

As was stated in Sec. I, the decay of magnetization to a final value corresponds to a creation of dipolar order which may be experimentally observed. In order to get a better description of the mixing process than in the one-temperature concept, let us project on the Zeeman and the dipolar variables

$$P = P_x + P_D = \frac{|\mathfrak{C}_x\rangle\langle\mathfrak{C}_x|}{(\mathfrak{C}_x|\mathfrak{C}_x)} + \frac{|\mathfrak{C}_{DZ}\rangle\langle\mathfrak{C}_{DZ}|}{(\mathfrak{C}_{DZ}|\mathfrak{C}_{DZ})}, \quad (2.28)$$

so that

$$\rho(t) = 1 - \alpha(t)\mathfrak{C}_x - \beta(t)\mathfrak{C}_{DZ} + \dots, \quad (2.29)$$

and therefore

$$\frac{d\alpha}{dt} = - \int_0^t K_{11}(t-t')\alpha(t') + K_{12}(t-t')\beta(t') dt', \quad (2.30a)$$

$$\frac{d\beta}{dt} = - \int_0^t K_{21}(t-t')\alpha(t') + K_{22}(t-t')\beta(t') dt', \quad (2.30b)$$

with

$$\begin{aligned} K_{11}(t) &= \frac{(\mathfrak{C}_x|\hat{\mathfrak{C}}_{DZ}\hat{S}(t)\hat{\mathfrak{C}}_{DZ}|\mathfrak{C}_x)}{(\mathfrak{C}_x|\mathfrak{C}_x)}, \\ K_{12}(t) &= -K_{11}(t), \\ K_{21}(t) &= -\frac{\omega_1^2}{\omega_L^2}K_{11}(t), \\ K_{22}(t) &= +\frac{\omega_1^2}{\omega_L^2}K_{11}(t), \end{aligned} \quad (2.31)$$

$$K_{11}(t) = M_2 \left[1 - \frac{t^2}{2} \left(\frac{M_4 - M_2^2}{M_2} + \omega_1^2 \right) + \frac{t^4}{4!} \left(\frac{M_6 - 2M_4M_2 + M_2^3}{M_2} + 2\omega_1^2 \frac{M_4 - M_2^2}{M_2} + 16\omega_1^2 \frac{\tilde{M}_4}{M_2} + \omega_1^4 \right) \dots \right]. \quad (2.36)$$

In order to determine the functional structure we consider again the "free" propagator

$$S_{\text{free}}(t) = e^{-it(1-P)\mathfrak{C}_x}. \quad (2.37)$$

It should be warned against the tempting approach to take $\exp(it\mathfrak{C}_x)$ as a "free" propagator, because this does *not* guarantee a systematic expansion in powers of ω_1 (low-field case) or ω_1^{-1} (high-field case). With Eq. (2.37) we obtain for the memory function

$$K_{\text{free}}(t) = M_2 \cos(\omega_1 t). \quad (2.38)$$

We now investigate again the damping function $g(t)$.

(i) Low-field case: BCH approximation

$$\begin{aligned} \exp[-it(1-P)\mathfrak{C}] &\approx \exp[-it(1-P_D)\mathfrak{C}_x] \\ &\quad \times \exp[-it(1-P_x)\mathfrak{C}_{DZ}] \\ &\quad \times \exp\left\{ \frac{t^2}{2} [(1-P_D) \right. \\ &\quad \left. \times \mathfrak{C}_x, (1-P_x)\mathfrak{C}_{DZ}] \right\} \end{aligned}$$

so that the Eqs. (2.30a) and (2.30b) may be reduced to one for the difference

$$\Delta(t) = \alpha(t) - \beta(t), \quad (2.32)$$

which reads

$$\frac{d}{dt}\Delta = - \int_0^t \left(1 + \frac{\omega_1^2}{\omega_L^2} \right) K_{11}(t-t')\Delta(t') dt'. \quad (2.33)$$

Obviously the energy

$$\Sigma = \alpha(t) + \frac{\omega_1^2}{\omega_L^2}\beta(t) \quad (2.34)$$

is a constant of motion

$$\frac{d}{dt}\Sigma = 0. \quad (2.35)$$

We want to emphasize that in the two-temperature concept employed here [Eqs. (2.30a) and (2.30b)] the thermodynamic limit (1.5) is self-consistently taken care of when $K_{11}(t)$ decays to zero. Also from the physical intuition the two-temperature concept is superior to the one-temperature concept.

Our aim is now to compute $K_{11}(t)$. First we consider again its moment expansion

which yields

$$K(t) = M_2 \left[1 - \frac{M_4 - M_2^2}{M_2} \frac{t^2}{2} \right] \cos(\omega_1 t). \quad (2.39)$$

(ii) High-field case: Magnus approximation. We obtain $\mathfrak{C}_0 = 0$, which leads to

$$K(t) = M_2 \cos(\omega_1 t),$$

as in the case of the "free" propagator, Eq. (2.38). We will come back to this astonishing result later.

D. Three-temperature concept

As has already been stated in the Introduction, for high fields ($\omega_1 \gg \omega_L$) there is a different behavior of secular and nonsecular dipolar interaction. Mixing takes place in two steps: (i) First the Zeeman reservoir and the nonsecular dipolar reservoir mix in a time of the order T_2 . (ii) Then this combined reser-

voir mixes with the secular dipolar reservoir in a time that grows as $T_2 \exp(\omega_I^2/\omega_L^2)$.^{9,27} Taking this different behavior of secular and nonsecular dipolar order into account, we project on three different relevant variables

$$\begin{aligned} P &= P_x + P_{DX} + P_{DDX} \\ &= \frac{|\mathfrak{C}_x\rangle\langle\mathfrak{C}_x|}{\langle\mathfrak{C}_x|\mathfrak{C}_x\rangle} + \frac{|\mathfrak{C}_{DX}/2\rangle\langle\mathfrak{C}_{DX}/2|}{\langle\mathfrak{C}_{DX}/2|\mathfrak{C}_{DX}/2\rangle} \\ &\quad + \frac{|\mathfrak{C}_{DZ} + \mathfrak{C}_{DX}/2\rangle\langle\mathfrak{C}_{DZ} + \mathfrak{C}_{DX}/2|}{\langle\mathfrak{C}_{DZ} + \mathfrak{C}_{DX}/2|\mathfrak{C}_{DZ} + \mathfrak{C}_{DX}/2\rangle}, \end{aligned} \quad (2.40)$$

where

$$[\mathfrak{C}_x, \mathfrak{C}_{DX}] = 0, \quad (2.41)$$

so that

$$\begin{aligned} \rho(t) &= 1 - \alpha(t)\mathfrak{C}_x - \beta(t)(-\mathfrak{C}_{DX}/2) \\ &\quad - \gamma(t)(\mathfrak{C}_{DZ} + \mathfrak{C}_{DX}/2) + \dots, \end{aligned} \quad (2.42)$$

and the equations of motion now read

$$\begin{aligned} \frac{d\alpha}{dt} &= - \int_0^t K_{11}(t-t')\alpha(t') + K_{12}(t-t')\beta(t') \\ &\quad + K_{13}(t-t')\gamma(t') dt', \end{aligned} \quad (2.43a)$$

$$\begin{aligned} \frac{d\beta}{dt} &= - \int_0^t K_{21}(t-t')\alpha(t') + K_{22}(t-t')\beta(t') \\ &\quad + K_{23}(t-t')\gamma(t') dt', \end{aligned} \quad (2.43b)$$

$$\begin{aligned} \frac{d\gamma}{dt} &= - \int_0^t K_{31}(t-t')\alpha(t') + K_{32}(t-t')\beta(t') \\ &\quad + K_{33}(t-t')\gamma(t') dt'. \end{aligned} \quad (2.43c)$$

Of these nine memory functions only three are really independent, due to symmetry Eq. (2.11) and completeness Eq. (2.13). We choose

$$K_{11}(t) = \frac{\langle\mathfrak{C}_x|\hat{\mathfrak{C}}_{DZ}\hat{S}(t)\hat{\mathfrak{C}}_{DZ}|\mathfrak{C}_x\rangle}{\langle\mathfrak{C}_x|\mathfrak{C}_x\rangle}, \quad (2.44a)$$

$$K_{12}(t) = \frac{\langle\mathfrak{C}_x|\hat{\mathfrak{C}}_{DZ}\hat{S}(t)\hat{\mathfrak{C}}_{DZ} - \mathfrak{C}_{DX}/2\rangle}{\langle\mathfrak{C}_x|\mathfrak{C}_x\rangle}, \quad (2.44b)$$

$$K_{22}(t) = \frac{\langle\mathfrak{C}_{DX}/2|\hat{\mathfrak{C}}_{DZ}\hat{S}(t)\hat{\mathfrak{C}}_{DZ}|\mathfrak{C}_{DX}/2\rangle}{\langle\mathfrak{C}_{DX}/2|\mathfrak{C}_{DX}/2\rangle}, \quad (2.44c)$$

and the rest may be calculated from these:

$$K_{13}(t) = -K_{11}(t) - K_{12}(t),$$

$$K_{21}(t) = \frac{4\omega_I^2}{\omega_L^2} K_{12}(t),$$

$$K_{23}(t) = -K_{21}(t) - K_{22}(t),$$

$$K_{31}(t) = \frac{4}{3} \frac{\omega_I^2}{\omega_L^2} K_{13}(t),$$

$$K_{32}(t) = \frac{1}{3} K_{23}(t),$$

$$K_{33}(t) = -K_{31}(t) - K_{32}(t).$$

We start with the moment expansion

$$K_{11}(t) = M_2 \left[1 - \frac{t^2}{2} \frac{M_4 - M_2^2}{M_2} + \frac{t^4}{4!} \left[\frac{M_6 - 2M_4M_2 + M_2^3}{M_2} + 4\omega_I^2 \frac{\tilde{M}_4}{M_2} \right] \dots \right], \quad (2.45a)$$

$$K_{12}(t) = -\frac{t^2}{2} \tilde{M}_4 + \dots, \quad (2.45b)$$

$$K_{22}(t) = \frac{3\tilde{M}_4}{M_2} - \dots. \quad (2.45c)$$

$K_{11}(t)$ and $K_{22}(t)$ are bounded by their initial values

$$|K_{11}(t)| \leq K_{11}(0), \quad (2.46a)$$

$$|K_{22}(t)| \leq K_{22}(0), \quad (2.46b)$$

whereas

$$|K_{12}(t)| \leq (M_2 \tilde{M}_4 / 4\omega_I^2)^{1/2}, \quad (2.46c)$$

so we see that for $\omega_I \rightarrow \infty$ K_{12} is of vanishing importance.

In order to determine the functional structure of the memory functions we consider first the "free" propagator

$$S_{\text{free}}(t) = \exp[-it(1 - P_{DDX})\mathfrak{C}_x],$$

which yields

$$K_{11}^{\text{free}}(t) = M_2, \quad (2.47a)$$

$$K_{12}^{\text{free}}(t) = 0, \quad (2.47b)$$

$$K_{22}^{\text{free}}(t) = \frac{3\tilde{M}_4}{M_2} \cos(2\omega_1 t). \quad (2.47c)$$

We now turn to the calculation of the damping functions. Starting with $K_{11}(t)$ we obtain

(i) low-field case: BCH approximation

$$K_{11}(t) = M_2 \left[1 - \frac{M_4 - M_2^2}{M_2} \frac{t^2}{2} + \dots \right],$$

(ii) high-field case: Magnus approximation

$$K_{11}(t) = M_2 \left[1 - \frac{M_4 - \tilde{M}_4 - M_2^2}{M_2} \frac{t^2}{2} + \dots \right].$$

The damping of $K_{12}(t)$ and $K_{22}(t)$ is not simply calculable since it involves the determination of higher moments analogous to the calculation of the sixth moment of the fid line shape.

We therefore make the following reasonable assumptions: (i) $\omega_1 \leq \omega_L$. $K_{12}(t)$ and $K_{22}(t)$ have the same damping constant as $K_{11}(t)$. (ii) $\omega_1 \gg \omega_L$. $K_{22}(t)$ has the same damping constant as $K_{11}(t)$, whereas $K_{12}(t) = 0$. This is formally justified by Eqs. (2.46c) and (2.47b) and physically reasonable since $K_{12}(t)$ describes the mixing between Zeeman and secular dipolar order whose rate decreases drastically as ω_1 increases. Together with the Gaussian functional assumption we finally obtain for $\omega_1 \leq \omega_L$:

$$K_{11}(t) = M_2 \exp \left[-\frac{M_4 - M_2^2}{M_2} \frac{t^2}{2} \right], \quad (2.48a)$$

$$K_{12}(t) = -\tilde{M}_4 \frac{t^2}{2} \exp \left[-\frac{M_4 - M_2^2}{M_2} \frac{t^2}{2} \right], \quad (2.48b)$$

$$K_{22}(t) = \frac{3\tilde{M}_4}{M_2} \exp \left[\frac{M_4 - M_2^2}{M_2} \frac{t^2}{2} \right] \cos(2\omega_1 t), \quad (2.48c)$$

and for $\omega_1 \gg \omega_L$:

$$K_{11}(t) = M_2 \exp \left[-\frac{M_4 - \tilde{M}_4 - M_2^2}{M_2} \frac{t^2}{2} \right], \quad (2.49a)$$

$$K_{12}(t) = 0, \quad (2.49b)$$

$$K_{22}(t) = \frac{3\tilde{M}_4}{M_2} \exp \left[-\frac{M_4 - \tilde{M}_4 - M_2^2}{M_2} \frac{t^2}{2} \right] \cos(2\omega_1 t). \quad (2.49c)$$

E. Nonsecular two-temperature concept

In the last section we noted that for $\omega_1 \gg \omega_L$ the thermodynamic coordinate $\beta(t)$ of the secular dipolar reservoir is an irrelevant variable for the first stage of the mixing process. It should therefore be sufficient for some T_2 to consider only Zeeman and nonsecular dipolar order as relevant variables, which leads to the following nonsecular two-temperature concept:

$$\begin{aligned} P &= P_x + P_{DDX} \\ &= \frac{|\mathcal{J}_x|(\mathcal{J}_x)}{(\mathcal{J}_x|\mathcal{J}_x)} + \frac{|\mathcal{J}_{DZ} + \mathcal{J}_{DX}/2|(\mathcal{J}_{DZ} + \mathcal{J}_{DX}/2)}{(\mathcal{J}_{DZ} + \mathcal{J}_{DX}/2|\mathcal{J}_{DZ} + \mathcal{J}_{DX}/2)} \end{aligned} \quad (2.50)$$

Therefore

$$\rho(t) = 1 - \alpha(t)\mathcal{J}_x - \gamma(t)(\mathcal{J}_{DZ} + \mathcal{J}_{DX}/2), \quad (2.51)$$

and

$$\frac{d\alpha}{dt} = - \int_0^t K_{11}(t-t')\alpha(t') + K_{13}(t-t')\gamma(t') dt', \quad (2.52a)$$

$$\frac{d\gamma}{dt} = - \int_0^t K_{31}(t-t')\alpha(t') + K_{33}(t-t')\gamma(t') dt'. \quad (2.52b)$$

The four memory functions resemble those of the three-temperature concept except for the changed projection operators. If we retain only the leading terms in ω_1 , we obtain

$$K_{13}(t) = -K_{11}(t),$$

$$K_{31}(t) = -\frac{4}{3} \frac{\omega_1^2}{\omega_L^2} K_{11}(t),$$

$$K_{33}(t) = +\frac{4}{3} \frac{\omega_1^2}{\omega_L^2} K_{11}(t),$$

and the two equations of motions [(2.52a) and (2.52b)] may be reduced to one for

$$\square(t) = \alpha(t) - \gamma(t), \quad (2.53)$$

$$\frac{d\square}{dt} = - \int_0^t \left[1 + \frac{4}{3} \frac{\omega_1^2}{\omega_L^2} \right] K_{11}(t-t')\square(t') dt',$$

where $K_{11}(t)$ is the same as in the three-temperature concept [see Eq. (2.44a)].

Once the Zeeman and the nonsecular dipolar reservoir are in equilibrium with each other (a process which has misleadingly been called "establishment of a Zeeman temperature" by several authors^{2,9}) it is tempting to describe also the second stage of the Zeeman-dipolar cross relaxation by a two-temperature concept.

After some T_2 we have for high fields

$$\rho_0 \approx 1 - \alpha_0^*(\mathcal{J}_x + \mathcal{J}_{DZ} + \mathcal{J}_{DX}/2) - \beta_0(-\mathcal{J}_{DX}/2), \quad (2.54)$$

where α_0^* is given by

$$\alpha_0^* = \alpha_0 \frac{\omega_1^2}{\omega_1^2 + 0.75\omega_L^2},$$

and $\beta_0 \ll \alpha_0^*$, which evolves into the final state

$$\rho_f = 1 - \alpha_f(\mathcal{J}_x + \mathcal{J}_{DZ}). \quad (2.55)$$

So we consider the following two-temperature concept

$$\begin{aligned} \rho(t) &= 1 - \alpha^*(t)(\mathcal{J}_x + \mathcal{J}_{DZ} + \mathcal{J}_{DX}/2) \\ &\quad - \beta(t)(-\mathcal{J}_{DX}/2) + \dots \end{aligned} \quad (2.56)$$

Hence

$$P = P_1 + P_2 = \frac{|\mathfrak{C}_x + \mathfrak{C}_{DZ} + \mathfrak{C}_{DX}/2|(\mathfrak{C}_x + \mathfrak{C}_{DZ} + \mathfrak{C}_{DX}/2)}{(\mathfrak{C}_x + \mathfrak{C}_{DZ} + \mathfrak{C}_{DX}/2)|\mathfrak{C}_x + \mathfrak{C}_{DZ} + \mathfrak{C}_{DX}/2|} + \frac{|\mathfrak{C}_{DX}/2|(\mathfrak{C}_{DX}/2)}{(\mathfrak{C}_{DX}/2)|\mathfrak{C}_{DX}/2|}, \quad (2.57)$$

and therefore

$$\frac{d\alpha^*}{dt} = - \int_0^t K_{\alpha\alpha}(t-t')\alpha^*(t') + K_{\alpha\beta}(t-t')\beta(t') dt', \quad (2.58a)$$

$$\frac{d\beta}{dt} = - \int_0^t K_{\beta\alpha}(t-t')\alpha^*(t') + K_{\beta\beta}(t-t')\beta(t') dt'. \quad (2.58b)$$

It may easily be seen that

$$K_{\beta\beta}(t) = K_{22}(t)$$

of Eq. (2.44c) and

$$K_{\beta\alpha}(t) = -K_{\alpha\beta}(t),$$

$$K_{\alpha\alpha}(t) = \frac{0.25\omega_L^2}{\omega_1^2 + 0.75\omega_L^2} K_{\beta\beta}(t),$$

$$K_{\alpha\beta}(t) = -K_{\alpha\alpha}(t),$$

so that

$$\frac{d}{dt} [\alpha^*(t) - \beta(t)] = - \int_0^t \left[\frac{\omega_1^2 + \omega_L^2}{\omega_1^2 + 0.75\omega_L^2} \right] K_{22}(t-t') \times [\alpha^*(t') - \beta(t')] dt'. \quad (2.59)$$

For times $t \gg T_2$, we may apply the short-correlation limit

$$\frac{d}{dt} [\alpha^*(t) - \beta(t)] \approx - \int_0^\infty \left[\frac{\omega_1^2 + \omega_L^2}{\omega_1^2 + 0.75\omega_L^2} \right] K_{22}(t') dt' \times [\alpha^*(t) - \beta(t)]. \quad (2.60)$$

Let us now consider the ω_1 dependence of the cross-relaxation rate. Since the damping function $g(t)$ of $K_{22}(t)$ was assumed to be Gaussian in Sec. III D, i.e.,

$$K_{22}(t) = \frac{3\tilde{M}_4}{M_2} \exp\left[-\frac{a}{2}t^2\right] \cos(2\omega_1 t),$$

we see that

$$\int_0^\infty \left[\frac{\omega_1^2 + \omega_L^2}{\omega_1^2 + 0.75\omega_L^2} \right] K_{22}(t') dt' \sim \exp(c\omega_1^2) + O(\omega_1^{-2}), \quad (2.61)$$

which reaffirms Kronig and Bouwkamp's result of 1938.²⁷

F. Related experiment of Jeener, Du Bois, and Broekaert

Jeener and co-workers⁸ performed an experiment that is very similar to spin locking except the fact that they started with high dipolar order

$$\rho_0 = 1 - \beta_0 \mathfrak{C}_{DZ}. \quad (2.62)$$

Under the irradiation of a strong rf field ($\omega_1/\omega_L = 4.37$) the nonsecular dipolar reservoir mixes with the Zeeman reservoir to a common temperature

$$\beta_f = \frac{0.75\omega_L^2}{\omega_1^2 + 0.75\omega_L^2} \beta_0. \quad (2.63)$$

The created Zeeman order alone is unobservable in this experiment. One nevertheless observes a decay of the dipolar order from β_0 to $\frac{1}{4}\beta_0$ which stems from the fact that the *secular* dipolar part does not mix in a time T_2 , so that after the rf pulse

$$\rho_f \approx 1 - \beta_0(-\mathfrak{C}_{DX}/2) \quad (2.64)$$

which decays into

$$\rho_\infty \approx 1 - \frac{1}{4}\beta_0 \mathfrak{C}_{DZ} \quad (2.65)$$

after some more T_2 . This has been discussed by Goldman.²

Our projection operator formalism now shows some peculiarities when we do not project on \mathfrak{C}_{DZ} but only on the relevant part which is $\mathfrak{C}_{DZ} + \mathfrak{C}_{DX}/2$, i.e.,

$$P = P_{DDX} = \frac{|\mathfrak{C}_{DZ} + \mathfrak{C}_{DX}/2|(\mathfrak{C}_{DZ} + \mathfrak{C}_{DX}/2)}{(\mathfrak{C}_{DZ} + \mathfrak{C}_{DX}/2)|\mathfrak{C}_{DZ} + \mathfrak{C}_{DX}/2|}, \quad (2.66)$$

$$\rho(t) = 1 - \gamma(t)(\mathfrak{C}_{DZ} + \mathfrak{C}_{DX}/2). \quad (2.67)$$

Now the second term in our equation of motion (2.8) does *not* vanish but yields

$$\frac{d\gamma}{dt} = -i \frac{(\mathfrak{C}_{DZ} + \mathfrak{C}_{DX}/2|\hat{\mathfrak{C}}\hat{S}(t,0)(1-P)|\rho(0))}{0.75(\mathfrak{C}_{DZ}|\mathfrak{C}_{DZ})} - \int_0^t K_{33}(t-t')\gamma(t') dt'. \quad (2.68)$$

This is a consequence of the fact that the initial state (2.62) is *not* completely in our projected subspace. One may, however, easily see that the first term on the right-hand side of Eq. (2.68) may be written as

$$-i \frac{(\mathfrak{C}_{DZ} + \mathfrak{C}_{DX}/2|\hat{\mathfrak{C}}\hat{S}(t,0)(1-P)|\rho(0))}{0.75(\mathfrak{C}_{DZ}|\mathfrak{C}_{DZ})} = - \int_0^t K_{32}(t') dt',$$

which corresponds to a $\beta(t) = \beta(t=0)$ in the three-temperature concept. The same effect arises in a

modified two-temperature concept for $\alpha(t)$ and $\gamma(t)$ as in Sec. IIE above, and only vanishes in the three-temperature concept, where the initial state (2.62) lies completely in the projected subspace.

III. EXPERIMENTAL RESULTS AND DISCUSSION

A. Experimental remarks

All experiments were performed on the ^{19}F spins in CaF_2 in a field of 2.114 T (84.6 MHz) at room temperature. The applied pulse sequence is shown in Fig. 1. After the 90°_y pulse the magnetization is "locked" by a spin-locking pulse of intensity H_{1x} and length τ as explained in the Introduction.

The initial height of the fid signal after this pulse was observed as a function of H_{1x} and τ . It represents the Zeeman order. In order to measure the dipolar order we then wait for a time of several T_2 and apply a 45°_x pulse. This produces a signal whose height is directly proportional to dipolar order.⁷ Unfortunately one cannot observe secular and nonsecular order, $\beta(\tau)$ and $\gamma(\tau)$, separately using this pulse sequence; instead one observes after some T_2 the weighted sum

$$\delta = 0.25\beta + 0.75\gamma \quad (3.1)$$

due to the different heat capacities of $\mathfrak{C}_{DX}/2$ and $\mathfrak{C}_{DZ} + \mathfrak{C}_{DX}/2$.²⁸

B. Low-field case

In order to check our theoretical results we now consider the spin locking in low field ($\omega_1 \leq \omega_L$) case. One special case is $\omega_1 = 0$, i.e., the free-induction decay (fid). In this case the one-temperature, two-temperature, and three-temperature concept all predict the Zeeman order to decay to zero:

$$\frac{d\alpha}{dt} = - \int_0^t K(t-t')\alpha(t')dt', \quad (3.2)$$

where

$$K(t) = M_2 \left[1 - \frac{M_4 - M_2^2}{M_2} \frac{t^2}{2} + \frac{M_6 - 2M_4M_2 + M_2^3}{M_2} \frac{t^4}{4!} \dots \right]$$

may be approximated as

$$K(t) = M_2 \exp\left[-\frac{M_4 - M_2^2}{M_2} \frac{t^2}{2}\right].$$

This explains quantitatively the experimental results of the fid up to the first zero and then at least qualitatively agrees with experiment [see Fig. 2(a) and Ref. 29].

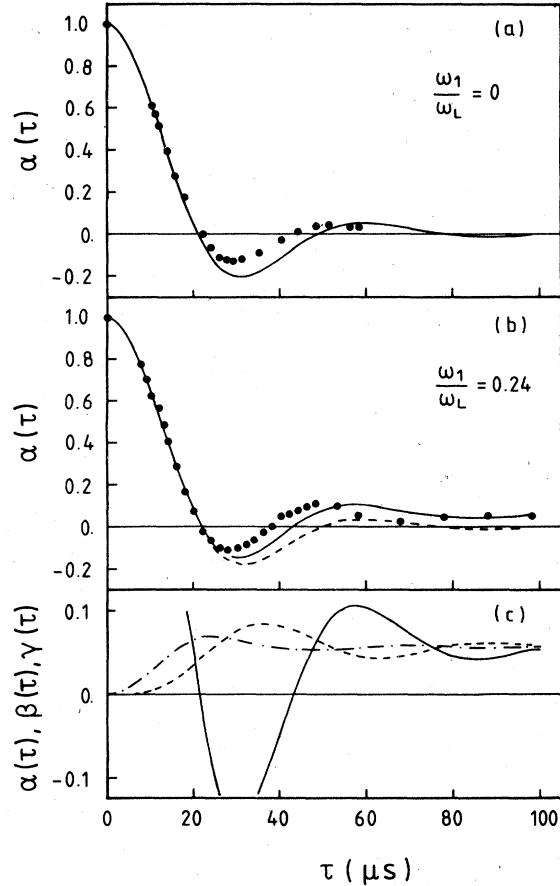


FIG. 2. (a) Free-induction decay of ^{19}F spins in CaF_2 with $H_0 \parallel [100]$. Dots represent data of Barnaal and Lowe (Ref. 29), solid line is $\alpha(\tau)$ as obtained from our theory with a Gaussian memory function. (b) Zeeman order $\alpha(\tau)$ as a function of τ for low-field case ($\omega_1/\omega_L = 0.24$, $H_0 \parallel [100]$). Dots are our experimental values; dashed line: one-temperature theory; solid line: two- and three-temperature theory. (c) Equilibration of Zeeman order (solid line), secular (dashed line), and nonsecular (dot-dashed line) dipolar order, calculated from three-temperature theory for $\omega_1/\omega_L = 0.24$, $H_0 \parallel [100]$.

This, however, is not surprising since the fid line shape may be fitted with almost every memory function line shape.^{11,13,17,26,30} If we now irradiate with a small rf field, the Zeeman order will not decay to zero, but will be locked at the value of Eq. (1.5), i.e.,

$$\alpha_f = \alpha_0 \frac{\omega_1^2}{\omega_1^2 + \omega_L^2}.$$

At the same time dipolar order builds up and approaches the same final temperature.

In the low-field case ($\omega_1 \leq \omega_L$) the two-temperature concept of Sec. IIC is sufficient to yield quantitative agreement with experiment, as may be seen from Figs. 2(b) and 3. In particular, the calculation

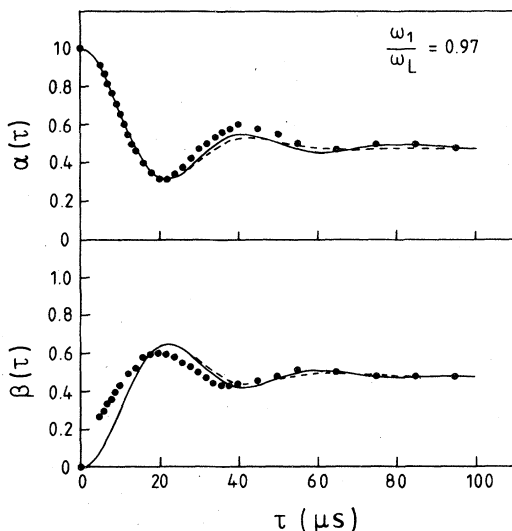


FIG. 3. Zeeman order $\alpha(t)$ and dipolar order $\beta(t)$ as a function of τ for the intermediate case ($\omega_1/\omega_L = 0.97$, $H_0 \parallel [100]$). Dots represent our experimental data; solid line: two-temperature theory; dashed line: three-temperature theory.

of the correlation functions in the three-temperature concept shows that secular and nonsecular dipolar order always remain in equilibrium with each other and relax with the Zeeman order on the same time scale [Fig. 2(c)].

C. High-field case

High-field spin-locking experiments provide much more phenomena than the low-field experiments, due to the fact that we now have three reservoirs and two relaxation times. We have calculated the thermodynamic coordinates $\alpha(t)$, $\beta(t)$, $\gamma(t)$ from Gauss-shaped memory functions using the one-temperature concept of Sec. II B, the three-temperature concept of Sec. II D and the nonsecular two-temperature concept of Sec. II E.

The comparison of our numerical calculations with our spin-locking experiments shows that only in the one-temperature concept we obtain quantitative agreement with experiment, whereas in the three- and nonsecular two-temperature concept we are only able to describe correctly the frequency of the oscillations and the shape of the curves up to the end of the first oscillation period (Fig. 4).

The most striking fact is that our numerical work predicts much weaker damping than do the experiments, where the oscillations are observed to die out in a time of the order of T_2 . Also the experiment of Jeener and co-workers⁸ shows this discrepancy. Figure 5 shows the measured values of $\delta = 0.25\beta + 0.75\gamma$

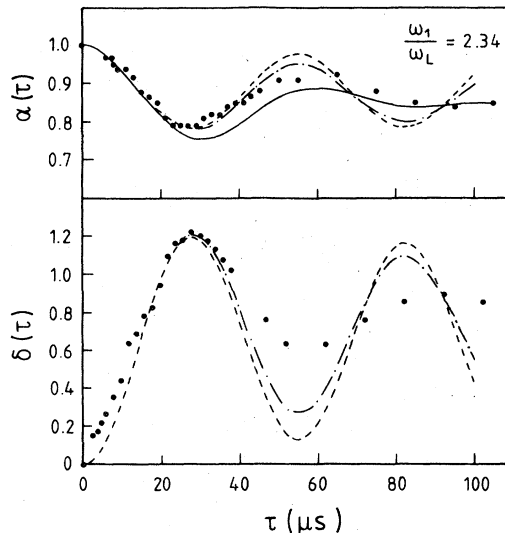


FIG. 4. Zeeman order $\alpha(\tau)$ and dipolar order $\delta(\tau) = 0.25\beta(\tau) + 0.75\gamma(\tau)$ as a function of τ for the high-field case ($\omega_1/\omega_L = 2.34$, $H_0 \parallel [111]$). Dots represent our experimental data; solid line: one-temperature theory; dashed line: nonsecular two-temperature theory; dot-dashed line: three-temperature theory.

[Eq. (3.1)] together with our calculations (note that in Fig. 2 of Ref. 22 an incorrect orientation of H_0 was used). In this case also the one-temperature concept (which had success in spin-locking experiments) fails to predict quantitatively correct damping.

Several explanations may be given for the disagreement between theory and experiment. One possibility, an instability of the numerical algorithm,²³ may be discarded since we have carefully checked its convergence properties; also the explanation that an inho-

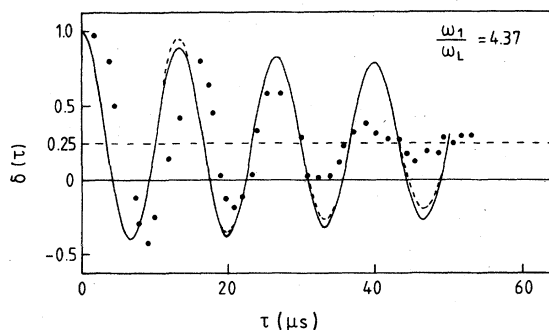


FIG. 5. Dipolar order $\delta(\tau) = 0.25\beta(\tau) + 0.75\gamma(\tau)$ in the experiment of Jeener and co-workers (Ref. 8) as a function of irradiation time ($\omega_1/\omega_L = 4.37$, $H_0 \parallel [100]$). Dots represent Jeener's data; solid line: one-temperature theory; dashed line: nonsecular two-temperature theory and three-temperature theory.

mogeneity of the rf field in the coil causes additional damping of the NMR signal does not seem to be the reason. We do believe that the discrepancy has its origin in the functional structure of the memory function which will be investigated in the next section.

D. Structure of the memory function

In this section we shall investigate some peculiarities of the memory functions in the spin-locking experiment. In the Secs. II B–II E we expanded the corresponding memory functions around the exactly solvable case of an undamped propagator, $S_{\text{free}}(t)$, and then tried to combine contributions from \mathfrak{C}_{DZ} in a damping function, $g(t)$, which was assumed to be of a simple form, e.g., Gaussian.

Two discrepancies between theory and experiment have already been observed.

(i) In the one-temperature concept of Sec. II B the Gaussian assumption for $g(t)$ was in conflict with the exact long-time behavior. In order to satisfy the latter requirement one must have (see Appendix A)

$$\int_0^{\infty} K(t) dt = 0 \quad (3.3)$$

exactly. Therefore the Gaussian form of $g(t)$ is only approximately correct in the high-field limit. Further application of the Mori continued fraction formalism¹² yields for the memory function of the memory function, $K_2(t)$

$$\frac{dK}{dt} = - \int_0^{\infty} K_2(t-t') K(t') dt' , \quad (3.4)$$

which leads to the following long-time behavior for $K_2(t)$

$$\lim_{t \rightarrow \infty} K_2(t) = 3\omega_1^2 , \quad (3.5)$$

so that $K_2(t)$ analogously to $G(t)$ possesses a pedestal. This is a functional form of a memory function which is completely new (to our belief) in the current literature. One might wonder if these difficulties are only present in the one-temperature concept and remedied by using a more refined projection operator, i.e., in our case going to a two-, modified two-, or three-temperature concept. Indeed these approaches automatically satisfy the correct thermodynamic limit as was already stated above. However, other complications arise, which are due to the unknown functional structure of the memory function.

(ii) Comparison with experimental data has shown that in the high-field limit the correct damping of the transient oscillations is not achieved by a Gaussian memory function, whereas the case of small fields up to $\omega_1 \approx \omega_L$ is very well represented. Since we have two different time scales for $\omega_1 \gg \omega_L$, the first being of the order of T_2 and governed by $K_{11}(t)$ (in the

three-temperature concept), while the second one is of the order of $T_2 \exp(\omega_1^2/\omega_L^2)$ and governed by $K_{22}(t)$, we restrict our consideration to an investigation of $K_{11}(t)$ which seems to be responsible for the lack of damping. First we want to point out that a Gaussian functional form for $K(t)$ does not automatically imply a Gaussian form for $G(t)$, but may, e.g., lead to a long-time exponential behavior as has been noted by Borckmans and Walgraef.¹¹

Now one could put the blame on the Gaussian assumption taken for the damping function $g(t)$ of $K_{11}(t)$ and try different functions also satisfying the symmetry and boundedness requirements and also possessing the correct second moment (see Appendix B). We found, however, that the other choices do not improve the damping significantly so that we are led to suspect that $g(t)$ is a “nonsimple” function. In order to clarify this proposal we consider the nonsecular two-temperature concept of Sec. II E and start from Eq. (2.53) for the difference of Zeeman and nonsecular dipolar order, $\square(t) = \alpha(t) - \gamma(t)$

$$\frac{d\square}{dt} = - \int_0^t \left[1 + \frac{4}{3} \frac{\omega_1^2}{\omega_L^2} \right] K_{11}(t-t') \square(t') dt' . \quad (2.53)$$

We now try to go the reverse way and calculate $K(t)$:

$$K(t) = \left[1 + \frac{4}{3} \frac{\omega_1^2}{\omega_L^2} \right] K_{11}(t)$$

from a $\square(t)$ that is assumed to be of Gaussian form, e.g.,

$$\square(t) = \exp(-\frac{1}{2} M_2 t^2) \cos(2\omega_1 t)$$

then we see that $K(t)$ is not Gaussian at all (Fig. 6) or Lorentzian or $(\sin t)/t$ or . . . , but decays to a (slowly decaying) intermediate quasiequilibrium value which becomes more pronounced as ω_1 increases. This may be understood as follows: Consider again the general equation of motion

$$\frac{d\square}{dt} = - \int_0^t K(t-t') \square(t') dt'$$

Laplace transformation leads to

$$\tilde{\square}(s) = \frac{\square(0)}{s + \tilde{K}(s)}$$

From this we get for $s=0$

$$\int_0^{\infty} \square(t) dt \int_0^{\infty} K(t) dt = \square(0) = 1 . \quad (3.6)$$

Now since we have chosen

$$\square(t) = \exp(-\frac{1}{2} M_2 t^2) \cos(2\omega_1 t) ,$$

we have

$$\int_0^{\infty} \square(t) dt = \left[\frac{\pi}{2M_2} \right]^{1/2} \exp\left[-\frac{2\omega_1^2}{M_2} \right] .$$

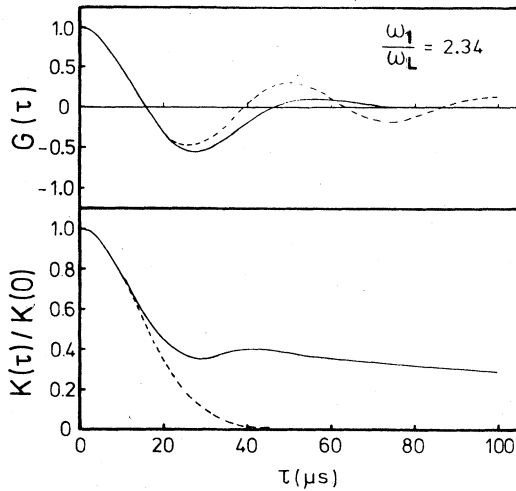


FIG 6. Numerical determination of $K(\tau)$ from a Gauss-shaped, cosine-modulated $G(\tau)$ according to Eq. (2.53) ($\omega_1/\omega_L = 2.34$, $H_0 \parallel [111]$ solid lines) and determination of $G(\tau)$ from a Gauss-shaped $K(\tau)$ with the correct second moment (dashed lines).

On the other hand

$$K(0) = \left[1 + \frac{4}{3} \frac{\omega_1^2}{\omega_L^2} \right] K_{11}(0)$$

only grows as ω_1^2 , so that in order to satisfy Eq. (3.6) the correlation time of $K(t)$ has to diverge. This seems to take place in more complicated manner, so that $K(t)$ seems to consist of two parts: a fast decaying (and oscillating) part and a slowly decaying contribution, both together leading to the complicated structure shown in Fig. 6. If one starts on the other hand with a Gaussian memory function possessing the correct second moment (dashed line) one obtains much weaker damping for $G(t)$.

Treating the exact equations of motion (2.8) in the so-called short-correlation limit (see Appendix C) yields some semiquantitative results in the high-field case. The ω_1 dependence of the second stage of the mixing process, however, is not known to sufficient accuracy at the present date although it is of vital interest for spin-lattice relaxation in the rotating frame as stated above.

IV. CONCLUSIONS

The memory function approach as applied here does offer a simple, but rigorous description of the oscillation behavior of macroscopic observables in a spin-locking experiment. Exact equations of motion have been set up for the different energies (or "inverse temperatures") involved and solved by use of

moment expansions and assumption of a functional form of the memory function, but without any free parameter.

One-, two-, and three-temperature concepts have been discussed and show progressive success in describing the dynamical behavior of the spin system under spin-locking conditions. Transients, which we observed experimentally, can be compared with theory quantitatively for relatively weak fields ($\omega_1 \leq \omega_L$), where in the case of high fields ($\omega_1 \gg \omega_L$) agreement between theory and experiment becomes worse. This has been traced back to the functional structure of the memory function which becomes of increasing importance in the high-field case.

A simple mathematical structure does not suffice and more elaborate techniques are required to yield correct interpretation of the experimental data. The theoretical technique described here has been applied to pulsed spin locking, too.²¹ This, however, will be published elsewhere.

ACKNOWLEDGMENTS

Financial support of part of this work by the Deutsche Forschungsgemeinschaft is gratefully acknowledged.

APPENDIX A: LONG-TIME BEHAVIOR OF $K(t)$ IN THE ONE-TEMPERATURE CONCEPT

We shall now derive some rigorous expansions for the long-time behavior of $K(t)$ in the one-temperature concept. Laplace transformation of Eq. (2.16) leads to

$$\tilde{\alpha}(s) = \frac{1}{s + \tilde{K}(s)}, \quad (\text{A1})$$

where $\tilde{\alpha}(s)$, $\tilde{K}(s)$ are the Laplace transforms of $\alpha(t)$, $K(t)$, respectively, and $\alpha(0) = 1$. In the long-time limit we have

$$\lim_{t \rightarrow \infty} \alpha(t) = \lim_{s \rightarrow 0} s \tilde{\alpha}(s) = \lim_{s \rightarrow 0} \frac{s}{s + \tilde{K}(s)} = \frac{\omega_1^2}{\omega_1^2 + \omega_L^2}, \quad (\text{A2})$$

where the last equality has its origin in the spin-thermodynamic results of Eq. (1.5). If we now assume that $\tilde{K}(s)$ may be expanded around $s = 0$, i.e.,

$$\tilde{K}(s) = \tilde{K}(0) + \tilde{K}'(0)s + \dots,$$

we immediately obtain from Eq. (A2) that

$$\tilde{K}(0) = 0, \quad \tilde{K}'(0) = \frac{\omega_1^2}{\omega_L^2}, \quad (\text{A3})$$

so that Eq. (3.3) follows,

In the same way, Laplace transformation of Eq. (3.4) leads to

$$\tilde{K}(s) = \frac{K(0)}{s + \tilde{K}_2(s)} . \quad (\text{A4})$$

Combining this with Eq. (A2) we obtain

$$\lim_{t \rightarrow \infty} K_2(t) = \lim_{s \rightarrow 0} s \tilde{K}_2(s) = 3\omega_1^2 ,$$

so that $K_2(t)$ possesses a pedestal.

APPENDIX B: FUNCTIONAL FORMS FOR $K_{11}(t)$

Let us recall the moment expansion for $K_{11}(t)$ [Eq. (2.45a)]

$$K_{11}(t) = M_2 \left[1 - \frac{N_2}{2} t^2 + \frac{N_4}{4!} t^4 \dots \right] ,$$

where

$$\begin{aligned} N_2 &= \frac{M_4 - M_2^2}{M_2} , \\ N_4 &= \frac{M_6 - 2M_4M_2 + M_2^3}{M_2} + 4\omega_1^2 \frac{\tilde{M}_4}{M_2} . \end{aligned} \quad (\text{B1})$$

We see that the ratio N_4/N_2^2 is strongly ω_1 dependent in contrast to possible one-parameter line shapes for $K_{11}(t)$, e.g.,

(i) sint/t

$$K_{11}(t) = M_2 \frac{\sin[(N_2/3)^{1/2}t]}{[(N_2/3)^{1/2}t]} , \quad N_4/N_2^2 = 1.8 ,$$

(ii) Gaussian

$$K_{11}(t) = M_2 \exp(-\frac{1}{2}N_2 t^2) , \quad N_4/N_2^2 = 3 ,$$

(iii) Lorentzian

$$K_{11}(t) = M_2 / (1 + \frac{1}{2}N_2 t^2) , \quad N_4/N_2^2 = 6 ;$$

so that the correct long-time behavior will not be reproduced by these choices for $K_{11}(t)$.

APPENDIX C: SHORT-CORRELATION LIMIT

The short-correlation limit of the equations of motion is capable of giving some semiquantitative results in the high-field case and is (at least in its simplest version) exactly calculable.

Let us start with the modified two-temperature concept of Sec. IIE and choose $K(t)$ to be exponential

$$K(t) = A \exp(-\alpha t) . \quad (\text{C1})$$

Then $\square(t)$ may be calculated exactly¹⁵ from Eq. (2.53)

$$\square(t) = \exp(-\frac{1}{2}\alpha t) \left[\cos(bt) + \frac{\alpha}{2b} \sin(bt) \right] , \quad (\text{C2})$$

with

$$b = \sqrt{A - \alpha^2/4} .$$

A and α may be determined if we expand $\tilde{K}(s)$ as a continued fraction

$$\tilde{K}(s) = \frac{(1 + \frac{4}{3}\omega_1^2/\omega_L^2)M_2}{s+} \frac{(M_4 - M_2^2)/M_2}{s+} \dots . \quad (\text{C3})$$

We then choose

$$A = \left[1 + \frac{4}{3} \frac{\omega_1^2}{\omega_L^2} \right] M_2 , \quad \alpha = \left[\frac{M_4 - M_2^2}{M_2} \right]^{1/2}$$

in order to terminate the continued fraction. If we insert this into Eq. (C2), we obtain $\square(t)$ with oscillations of the frequency $2\omega_1 + O(\omega_1^{-1})$ and a damping constant $\frac{1}{2}[(M_4 - M_2^2)/M_2]^{1/2}$ which is independent of ω_1 . This is a special feature of the exponential form of $K(t)$, since

$$\int_0^\infty \left[1 + \frac{4}{3} \frac{\omega_1^2}{\omega_L^2} \right] K_{11}(t) dt \sim \omega_1^2 ,$$

and from Eq. (C2)

$$\int_0^\infty \square(t) dt \sim \omega_1^{-2} ,$$

so that the ω_1 dependence exactly matches.

This simple model for $K_{11}(t)$ may also serve to consider the two relaxation times in the three-temperature concept. If we assume that $K_{22}(t)$ has the same exponential decay behavior with the same constant, we have in the short-correlation limit

$$\frac{d\alpha}{dt} = - \int_0^\infty K_{11}(t') dt' \alpha(t) + \int_0^\infty K_{11}(t') dt' \gamma(t) , \quad (\text{C4})$$

$$\frac{d\beta}{dt} = - \int_0^\infty K_{22}(t') dt' \beta(t) + \int_0^\infty K_{22}(t') dt' \gamma(t) , \quad (\text{C5})$$

$$\begin{aligned} \frac{d\gamma}{dt} &= \int_0^\infty \frac{4}{3} \frac{\omega_1^2}{\omega_L^2} K_{11}(t') dt' \alpha(t) + \int_0^\infty \frac{1}{3} K_{22}(t') dt' \beta(t) \\ &\quad - \int_0^\infty \left[\frac{4}{3} \frac{\omega_1^2}{\omega_L^2} K_{11}(t') + \frac{1}{3} K_{22}(t') \right] dt' \gamma(t) , \end{aligned} \quad (\text{C6})$$

which yields the following eigenvalues

$$\begin{aligned} \lambda_1 &= 0 \quad (\text{corresponding to conserved quantities}) , \\ \lambda_2, \lambda_3 &< 0 , \end{aligned}$$

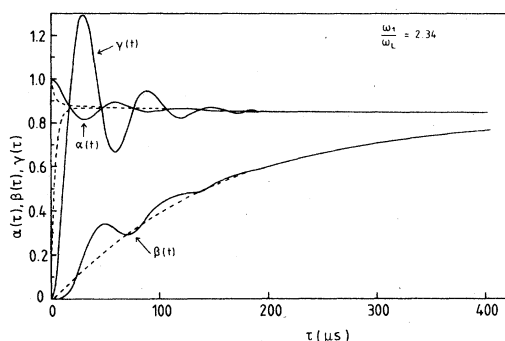


FIG. 7. Numerical calculation of $\alpha(\tau)$, $\beta(\tau)$, $\gamma(\tau)$ in the three temperature concept with exponential memory functions [Eq. (2.43), solid lines] and in the short-correlation limit [Eqs. (C4)–(C6), dashed lines] in the high-field case ($\omega_1/\omega_L = 2.34$, $H_0 \parallel [111]$).

with

$$|\lambda_2| \propto \omega_1^2, \quad |\lambda_3| \propto \omega_1^{-2}.$$

Obviously λ_2 is the decay constant for the first step of the mixing process [it should in principle be ω_1 independent; the ω_1^2 dependence stems from the $\cos(2\omega_1 t)$ term], while λ_3 describes the second step of the mixing process.

We see in our model that in this second step the mixing process is rather well described by the equations of motion in the short-correlation limit, Eqs. (C4)–(C6) (Fig. 7). Other more realistic models show an even stronger ω_1 dependence of λ_3 . For example the assumption of a Gaussian cross-relaxation spectrum [Eq. (2.61)],^{9,31} yields

$$\lambda_3 \propto \exp(-c\omega_1^2)$$

and also a Lorentzian cross-relaxation function has been considered³² leading to

$$\lambda_3 \propto \exp(-c\omega_1).$$

¹A. Abragam, *The Principles of Nuclear Magnetism* (Oxford University Press, London, 1961).

²M. Goldman, *Spin Temperature and Nuclear Magnetic Resonance in Solids* (Oxford University Press, London, 1970).

³C. P. Slichter and D. Ailion, *Phys. Rev.* **135A**, 1099 (1964).

⁴R. L. Strombotne and E. L. Hahn, *Phys. Rev.* **133A**, 1616 (1964).

⁵W. K. Rhim, D. P. Burum, and D. D. Elleman, *Phys. Rev. Lett.* **37**, 1764 (1976); **39**, 850 (1977).

⁶I. Solomon, *C. R. Acad. Sci. (Paris)* **248**, 92 (1959).

⁷J. Jeener and P. Broekaert, *Phys. Rev.* **157**, 232 (1967).

⁸J. Jeener, R. Du Bois, and P. Broekaert, *Phys. Rev.* **139A**, 1959 (1965).

⁹P. Mansfield and D. Ware, *Phys. Rev.* **168**, 318 (1968).

¹⁰B. N. Provotorov, *Sov. Phys. JETP* **14**, 1126 (1962) [*Zh. Eksp. Teor. Fiz.* **41**, 1582 (1961)].

¹¹P. Borckmans and D. Walgraef, *Physica (Utrecht)* **35**, 80 (1967); *Phys. Rev.* **167**, 282 (1968); D. Walgraef and P. Borckmans, *ibid.* **187**, 421 (1969); P. Borckmans and D. Walgraef, *Phys. Rev. B* **7**, 563 (1973).

¹²H. Mori, *Prog. Theor. Phys.* **34**, 399 (1965).

¹³M. Engelsberg and I. J. Lowe, *Phys. Rev. B* **12**, 3547 (1975); M. Engelsberg and N. C. Chao, *ibid.* **12**, 5043 (1975).

¹⁴R. Zwanzig, *J. Chem. Phys.* **33**, 1338 (1960).

¹⁵H. Mori, *Prog. Theor. Phys.* **33**, 423 (1965).

¹⁶T. Shimizu, *J. Phys. Soc. Jpn.* **28**, 811 (1970).

¹⁷F. Lado, J. D. Memory, and G. W. Parker, *Phys. Rev. B* **4**, 1406 (1971).

¹⁸T. Shimizu, *J. Phys. Soc. Jpn.* **29**, 74 (1970); J. Stepisnik, *Phys. Rev. B* **7**, 3250 (1973); R. Blinc, J. Pirs, and S. Zumer, *ibid.* **8**, 15 (1973); D. E. Demco, J. Tegenfeld, and J. S. Waugh, *ibid.* **11**, 4133 (1975); M. Mehring and G.

Sinning, *ibid.* **15**, 2519 (1977).

¹⁹M. Mehring, "High Resolution NMR in Solids," *NMR: Basic Principles and Progress* (Springer, Berlin, 1976), Vol. 11.

²⁰According to Appendix E of Ref. 19, in most cases the system can be prepared in such a state that the first two terms on the right-hand side of Eq. (2.8) are zero. A counter example will be given, however, in Sec. IIF.

²¹U. Deininghaus, Diploma thesis (Dortmund, 1977) (unpublished).

²²U. Deininghaus and M. Mehring, *Phys. Lett.* **73A**, 129 (1979).

²³B. J. Berne and G. D. Harp, *Adv. Chem. Phys.* **17**, 63 (1970).

²⁴R. Wilcox, *J. Math. Phys.* **8**, 962 (1967).

²⁵P. Pechukas and J. C. Light, *J. Chem. Phys.* **44**, 3897 (1966); U. Haeberlen and J. S. Waugh, *Phys. Rev.* **175**, 453 (1968).

²⁶J. A. Tjon, *Phys. Rev.* **143**, 259 (1966); M. Tokuyama and H. Mori, *Prog. Theor. Phys.* **55**, 411 (1976).

²⁷R. de L. Kronig and C. J. Bouwkamp, *Physica (Utrecht)* **5**, 521 (1938); W. J. Caspers, *Physica (Utrecht)* **26**, 778 (1960); S. R. Hartmann and A. G. Anderson, in *Proceedings of the XIth Colloque Ampère, 1962* (North-Holland, Amsterdam, 1963); B. Sapoval and D. Lepine, *J. Phys. Chem. Solids* **27**, 115 (1966).

²⁸Experiment C of Ref. 8, however, is capable of measuring $\beta(\tau)$ and $\gamma(\tau)$ separately.

²⁹D. E. Barnaal and I. J. Lowe, *Phys. Rev.* **148**, 328 (1966).

³⁰P. Mansfield, *Phys. Rev.* **151**, 199 (1966); G. W. Parker and F. Lado, *Phys. Rev. B* **8**, 3081 (1973).

³¹R. E. Walstedt, *Phys. Rev.* **138A**, 1096 (1965); H. Stokes and D. C. Ailion, *Phys. Rev. B* **16**, 3056 (1977).

³²A. N. Garroway, *J. Magn. Reson.* **34**, 283 (1979).